Band offsets and optical bowings of chalcopyrites and Zn-based II-VI alloys

Su-Huai Wei[a] and Alex Zunger
National Renewable Energy Laboratory, Golden, Colorado 80401

(Received 20 December 1994; accepted for publication 2 June 1995)

Using first-principles band structure theory we have systematically calculated the (i) alloy bowing [illegible] for three mixed-anion ($CuMX_2$, X=S, Se, Te) and three mixed-cation ($CuMSe_2$, M=Al, Ga, In) chalcopyrite systems. The random chalcopyrite alloys are represented by special quasirandom structures (SQS). The calculated bowing coefficients are in good agreement with the most recent [illegible] offsets for the mixed-anion chalcopyrite alloys with those of the corresponding Zn chalcogenide alloys (ZnX, X=S, Se, Te), we find that the larger $p-d$ coupling in chalcopyrite alloys reduces their band offsets and optical bowing. Bowing parameters for ordered, Zn-based II-VI alloys in the CuAu, CuPt, and chalcopyrite structures are presented; we find that ordered ZnSeTe has bowing coefficients of 1.44 and 3.15 eV in the CuAu and CuPt structures, while the random $ZnSe_xTe_{1-x}$ alloy has a bowing of 1.14 eV. The band alignment between $CuInSe_2$ and $CuInSe_2$-derived ordered vacancy compounds are also presented. © *1995 American Institute of Physics.*

I. INTRODUCTION

$A_{1-x}B_x$ semiconductor alloys constitute a group of technologically important materials since their structural, transport, and optical properties can be tuned continuously by [illegible] properties available from the pure constituents A and B. For example, the band gaps $E_g(x)$ of $A_{1-x}B_x$ alloys can often be described by

where b is an "optical bowing coefficient." Figure 1 illustrates that alloys between different I-III-VI_2 chalcopyrites[1–4] offer a new, redshifted range of band gaps relative to the alloys of common II-VI compounds.[5,6] It has been shown [illegible] with $CuInS_2$ can increase the band gap of $CuInSe_2$, a change that increases the efficiency of thin-film $CuInSe_2$ solar cells.[9] In Table I we summarize the measured[10–33] bowing parameters of the Cu-based chalcopyrite alloys, while Table II give analogous results[34–41] for the Zn chalcogenide alloys. Table I [illegible] copyrite materials are known rather well, very little is known definitely about the properties of their *alloys*. In fact, measurements of optical bowing parameters are lacking for many Cu-III-VI_2 alloys with III=Al, Ga, In and VI=S, Se, Te and, in those cases where data are available, the scatter between different measurements on the same alloy is significant. In some cases, even the sign of the bowing parameter is under dispute, e.g., $CuIn(S,Se)_2$ and $Cu(Ga,In)Se_2$. Other properties, such as the band offsets between the chalcopyrite compounds (needed for device design),[9] are also generally unknown. From the point of view of fundamental physics, it is gaps of individual chalcopyrite compounds are significantly lower than those of the corresponding II-VI compounds [e.g., $E_g(CuGaX_2) < E_g(ZnX)$ for X=S, Se, Te; see Fig. 1][4] but also why the chalcopyrite *bowing parameters* (Tables I and II) and *valence-band offsets* (see below) are systematically [illegible] counterparts [e.g., $b(CuMS_{1-x}Se_x) < b(ZnS_{1-x}Se_x)$ and $b(CuMSe_{1-x}Te_x) < b(ZnSe_{1-x}Te_x)$].

In this paper we have calculated the (i) alloy bowing [illegible] mixed-cation $CuAlSe_2/CuGaSe_2/CuInSe_2$ and mixed-anion [illegible]

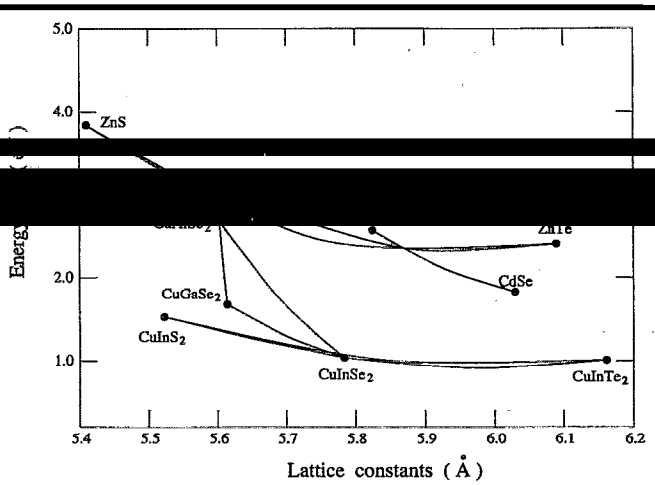

[illegible] (1) to describe band gaps as a function of composition x, while for the lattice constant we use Eq. (5). Experimental values (solid dots) are used for the end-point compounds (see Table IV below).

[a]Electronic mail: shw@nrel.gov

 0021-8979/95/78(5)/2846/11/$6.00

TABLE I. Measured optical bowing parameter b (in eV) of the [illegible]

System	b	Sample type	Growth method	Author (year)	Ref.
Mixed anion					
[illegible]	[illegible]	[illegible]	[illegible]	[illegible]	[illegible]
[illegible]	0.00	Single	Iodine chemical transport	[illegible]	[illegible]
	0.14	Single	Melt and anneal	Abid *et al.* (1987)	Ref. 17
	−0.02			Samanta *et al.* (1993)	Ref. 13
$CuAl(Se,Te)_2$					
$CuGa(Se,Te)_2$	0.22	Single	Melt and anneal	Avon *et al.* (1983)	Ref. 18
	0.34	Poly	Melt and anneal	Chatraphorn *et al.* (1985)	Ref. 19
	0.00			Samanta *et al.* (1993)	Ref. 13
$CuIn(Se,Te)_2$	0.39	Single	Melt and anneal	Avon *et al.* (1983)	Ref. 18
	0.35	Poly	Melt and anneal	Chatraphorn *et al.* (1985)	Ref. 19
	0.42	Poly	Melt and anneal	Quintero *et al.* (1991)	Ref. 20
	0.30			Samanta *et al.* (1993)	Ref. 13
$CuGa(S,Te)_2$	−0.30			Samanta *et al.* (1993)	Ref. 13
Mixed cation					
[illegible]	[illegible]	[illegible]	[illegible]	[illegible]	[illegible]
$Cu(Al,Ga)Se_2$	0.28	Single	Iodine chemical transport	Shirakata *et al.* (1993)	Ref. 23
$Cu(Al,Ga)Te_2$					
$Cu(Ga,In)S_2$	0.19	Single	Iodine chemical transport	Bodnar *et al.* (1986)	Ref. 24
	0.31	Single	Iodine chemical transport	Shirakata *et al.* (1993)	Ref. 12
	0.15			Samanta *et al.* (1993)	Ref. 13
	0.20			Samanta *et al.* (1993)	Ref. 13
$Cu(Ga,In)Se_2$	0.15	Single	Iodine chemical transport	Bodnar *et al.* (1982)	Ref. 25
	−0.07	Single	Melt and anneal	Avon *et al.* (1983)	Ref. 18
	0.03	Single	Melt and anneal	Abid *et al.* (1987)	Ref. 17
	0.16	Single	Bridgman	Ciszek *et al.* (1987)	Ref. 26
	0.16	Single	Bridgman	Durran (1987)	Ref. 27
	0.11	Poly	Evaporation	Dimmler *et al.* (1987)	Ref. 28
	0.14	Poly	Evaporation	Chen *et al.* (1987)	Ref. 29
	0.24	Poly	Evaporation	Albin *et al.* (1991)	Ref. 30
	0.15	Single	Chemical vapor deposition	Tinoco *et al.* (1991)	Ref. 31
	0.13	Poly	RF sputtering	Yamaguchi *et al.* (1992)	Ref. 32
	0.02	Single	Iodine chemical transport	Larez *et al.* (1994)	Ref. 33
	0.15			Samanta *et al.* (1993)	Ref. 13
	0.17			Samanta *et al.* (1993)	Ref. 13
	0.21			Samanta *et al.* (1993)	Ref. 13
$Cu(Ga,In)Te_2$	−0.22	Single	Melt and anneal	Avon *et al.* (1983)	Ref. 18
	−0.33			Samanta *et al.* (1993)	Ref. 13
$Cu(Al,In)S_2$					
$Cu(Al,In)Se_2$					
$Cu(Al,In)Te_2$					

ciples, self-consistent electronic structure theory based on the local density approximation[42] (LDA). Our principal results for the bowing parameters (b), the mixing enthalpy at $x=1/2$ (ΔH) and the valence-band offset (ΔE_v) are summarized in Fig. 2 for mixed-anion chalcogenides [illegible] and mixed-anion Zn chalcogenide alloys are given in Fig. 3. This paper describes how [illegible] discusses the significant physics of the results (Sec. III).

II. METHOD OF CALCULATION

A. Special quasirandom structures

A random alloy is distinguished from an ordered compound by the fact that the site occupations in the [illegible] for random alloys the site occupations are known only proba[illegible] structural model for random substitutional A_xB_{1-x} alloys is

TABLE II. Measured bowing parameters b (in eV) of the lowest gaps in Zn-based chalcogenide alloys. "Single" and "poly" refer to single crystal and polycrystalline, respectively.

System	b	Sample type	Growth method	Author (year)	Reference
Zn(S,Se)	0.41	Single	Melt and anneal	Suslina *et al.* (1977)	34
	0.63	Single	Chemical vapor deposition	Ebina *et al.* (1974)	35
	0.43	Single	Iodine chemical transport	Mach *et al.* (1982)	36
	0.55	Poly	Evaporation	Shazly *et al.* (1985)	37
Zn(Se,Te)	1.23	Single	Chemical vapor deposition	Ebina *et al.* (1972)	38
	1.51		molecular beam epitaxy	Brasil *et al.* (1991)	39
Zn(S,Te)	3.0	Poly	Evaporation	Hill *et al.* (1973)	40
	3.2		molecular beam epitaxy	Wong *et al.* (1994)	41

to consider a huge unit cell whose sites are occupied by A [illegible] (for mathematical convenience) periodic boundary conditions then gives a "pseudo-ordered crystal" that can be [illegible] sufficiently large "supercells" this approach becomes exact. In practice, this approach has been applied within the context of semiempirical electronic structure methods for ~2000 atom/cell, producing rather accurate results.[43–45] Despite the success of this direct method, this procedure requires a large [illegible] physically most relevant structural correlation functions $\Pi_{k,m}$ are forced to be closest to the exact values in an infinite

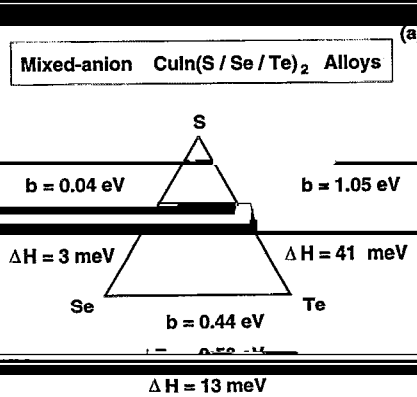

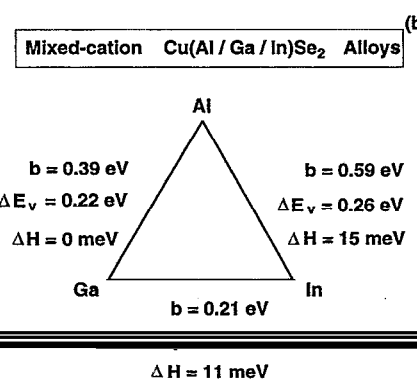

FIG. 2. Calculated bowing coefficients b, valence-band offsets ΔE_v, and alloy mixing energies ΔH at $x=1/2$ of (a) mixed-anion chalcopyrite alloys and (b) mixed-cation chalcopyrite alloys. ΔH is given in meV per atom. The value given in the figure should be multiplied by two to convert it to meV [illegible] should be multiplied by four.

computationally practical in conjunction with the highly accurate but mathematically complex first principles LDA band-structure methods. There is, however, a more efficient way to achieve practically the same result: we know that the [illegible] atomic structure, and that the structure can be quantified by the "structural correlation functions" $\bar{\Pi}_{k,m}$ for atomic clusters (k,m) with k vertices and up to mth neighbor.[46] Hence, rather than occupy sites of a huge unit cell *at random*, one can occupy sites of a "small" unit cell (the "special quasir-[illegible] are forced to be closest to the exact values in an infinite percells (~20 atoms) with correlation functions that approach the exact values in very large random supercells.

The SQS method has been previously applied to III-V[45,47,48] and II-VI[47,49] zinc-blende alloys as well as to fcc transition metal alloys.[50,51] The coordinates of these SQS can be found in these references (a more detailed description and a list of the SQS coordinates for the blende alloys can be obtained from the FTP site ftp://ftp.nrel.gov/pub/sst/archive/sqs). Here we apply the SQS method to alloys between chalcopyrites.

[illegible] $CuIn(S_{0.5}Se_{0.5})_2$], the anions occupy an fcc sublattice, hence, for the anion sublattice we can use the fcc SQS. The cation

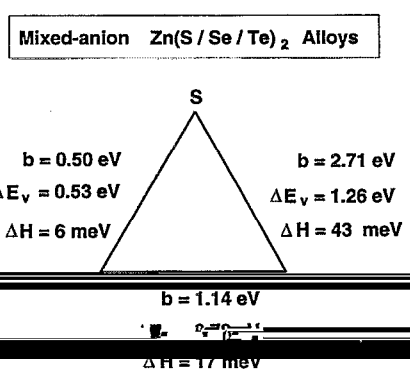

FIG. 3. Calculated bowing coefficients b, valence-band offsets ΔE_v, and alloy mixing energies ΔH at $x=1/2$ of mixed-anion chalcogenide alloys. [illegible] multiplied by two to convert it to meV per mixed-anion.

TABLE III. Structural correlation functions $\bar{\Pi}_{k,m}$ of the random alloys at $x=1/2$, where k is the number of vertices of the cluster ($k=2$ is pair, $k=3$ is

bors, respectively). For the mixed-cation SQS we use the notation of fcc

SQS (mixed cation)	0	0		−2/3	0	1/3	0	
Exact random	0	0	0	0	0	0	0	0

sublattice needs to have the chalcopyrite translational symmetry, so that the final SQS unit cell should be commensurate with both the chalcopyrite structure of the cation sublattice and with the SQS of the anion sublattice. This is achieved here using a sixteen atom SQS unit cell. It has the Cartesian lattice vectors:

$$\mathbf{a}_3=(2,2,0)\,\frac{a}{2}, \tag{2}$$

where a is the lattice constant and $\eta=c/2a$ is the tetragonal ratio. In this unit cell the anions form an fcc SQS4 (an A_2B_2 superlattice along the [110] direction).[49]

For Cu-based *mixed-cation chalcopyrite alloys* (e.g.

tered tetragonal lattice. The Cu sublattice has the chalcopyrite translational symmetry, while the anions occupy an fcc sublattice. In the present calculation, we used a 16-atom SQS cell (with four mixed atoms) which has the same lattice vectors as in Eq. (2). For unrelaxed $CuGa_{0.5}In_{0.5}Se_2$ alloy the

$$\mathrm{Cu}^{(1)}(0,0,0)\,\frac{a}{}; \quad \mathrm{Cu}^{(2)}(0,1,1)\,\frac{a}{}$$

$$\mathrm{Cu}^{(3)}(1,1,2)\,\frac{a}{2}; \quad \mathrm{Cu}^{(4)}(2,1,1)\,\frac{a}{2}, \tag{3}$$

$$\mathrm{Ga}^{(1)}(0,0,2)\,\frac{a}{}; \quad \mathrm{Ga}^{(2)}(1,0,1)\,\frac{a}{}$$

$$\mathrm{In}^{(1)}(1,1,0)\,\frac{a}{2}; \quad \mathrm{In}^{(2)}(1,2,1)\,\frac{a}{2}.$$

It is interesting to see that the mixed cations also form an A_2B_2 superlattice along the [110] direction. The structural correlation functions of these SQS are given in Table III; they are compared with the ideal random alloy correlation functions. We see that for both mixed-cation and mixed-anion alloys the first error of pair correlation functions oc-

cation-anion bonds with lengths given by

TABLE IV. Structural parameters and band gaps used in the present calculation for five pure chalcopyrite compounds and three Zn-based II-VI com-

rite compounds, except for $CuAlSe_2$, where we used our estimated internal

from Ref. 6. Our calculated LDA crystal field splitting Δ_{CF} and spin-orbit

System	a(Å)	$\eta=c/a$	u	E_g (eV)	Δ_{SO} (eV)	Δ_{CF} (eV)
$CuInSe_2$	5.784	1.004	0.224	1.04	0.184	−0.02
$CuInTe_2$	6.161	1.003	0.225	1.01	0.598	−0.00
ZnS	5.409	1.000	0.250	3.84	0.068	0.000
ZnSe	5.668	1.000	0.250	2.82	0.396	0.000
ZnTe	6.089	1.000	0.250	2.40	0.883	0.000

$$R_{BX}=a\left[\frac{1}{16}+\left(\frac{1}{2}-u\right)^2+\frac{\eta^2}{16}\right]^{1/2}, \tag{4}$$

where a is the lattice constant, $\eta=c/2a$ is the tetragonal ratio, and u is a dimensionless internal relaxation parameter. In the undistorted lattice $u=1/4$ and $\eta=1$, so $R_{AX}=R_{BX}=(\sqrt{3}/4)a$. In a *pure* chalcopyrite crystal the structure is determined once $\{a,\eta,u\}$ are specified. In a chal-

external structural parameters that need to be determined. It is crucial to find the equilibrium values of these parameters since band gaps depend on atomic relaxation.[4] Our first-principles total energy and force calculations show that for these rather ionic alloys the anion-cation bond lengths have

lengths"[4] indicates that the bond bending force[52,53] in chal-

relaxed atomic positions in our chalcopyrite SQS and superlattices of $(ABX_2)_n/(A'B'X_2')_n$ (Sec. II D) by requiring that (i) the nearest-neighbor anion-cation bond lengths in the alloy equal their respective values in the pure chalcopyrite

$$a(x)=(1-x)a_{ABX_2}+xa_{A'B'X_2'}. \tag{5}$$

These requirements uniquely determine all cell-internal and cell-external parameters of the model alloy.

The input[2,4] $\{a,u,\eta\}$ to our calculation is given in the first three columns of Table IV. Using these values for each chalcopyrite and Eq. (4) we determine the bond lengths in the *alloy*. In all cases but $CuAlSe_2$ we use measured

Sb) the Al–V bond length is slightly *longer*[6] (by 0.1%–

0.6%) than the Ga–V bond length, while in the ionic nitrides the Al–N bond length is about 3% *shorter* than the Ga–N

copyrite, we find that the Al–Se bond length is about 2% *smaller* than the Ga–Se bond. The difference between the In bond length and the Ga bond length are found to be similar

Using the unit cell structure of the SQS (Sec. II A) and the relaxed atomic positions (Sec. II B) we can now apply band-structure techniques to evaluate the alloy band gaps E_g

performed using the density functional formalism as implemented by the general potential, *relativistic*, all electron, linearized augmented plane wave (LAPW) method.[56] [Note that the earlier calculations of Jaffe and Zunger[3,4] were nonrelativistic.] We used the Ceperley–Alder exchange correlation

using special **k** points which are equivalent[57] to the ten spe-

The crystal field splitting $\Delta_{CF}=\varepsilon(\Gamma_{4v})-\varepsilon(\Gamma_{5v})$ is cal-

the tetragonal distortion $1-\eta$ increases.[4] This explains the

Our calculated Δ_{CF} are in good agreement with experimental data.[10,22,32]

culated fully relativistic band energies to the quasicubic

orbit splittings of the chalcopyrites are much smaller than the corresponding values in the II-VI Zn compounds. For

negative term to the spin-orbit splitting,[62–64] the larger mixtion of the spin-orbit splitting relative to II-VIs. This stronger

band gaps relative to their corresponding II-VI compounds (Table IV and Fig. 1).

D. Calculation of band offsets

To calculate the valence-band offset $\Delta E_v(ABX_2/A'B'X_2')$ at the interface between two chal-

in photoemission core-level spectroscopy, where the band offset is given by

$$\Delta E_v=\Delta E_v^{ABX_2}-\Delta E_v^{A'B'X_2'}+\Delta E_{\quad} \tag{6}$$

Here,

and

$$\Delta E_v^{A'B'X_2'}=E_v^{A'B'X_2'}-E_C^{A'B'X_2'} \tag{8}$$

are the core level to valence-band maximum energy separa-

$$\Delta E_{C,C'}=E_C^{ABX_2}-E_{C'}^{A'B'X_2} \tag{9}$$

is the difference in core-level binding energy between ABX_2

the core to VBM energy difference $\Delta E_{VBM,C}$ is obtained as an eigenvalue difference for each of the component chalcopyrites. We wish to obtain the band offset for a fully relaxed interface, where each component has its own equilibrium lattice parameter. Thus, the first two terms in Eq. (6) are calculated at their respective equilibrium structural param-

core-level difference $\Delta E_{C,C'}$ between the two chalcopyrites

are bulk like. We find that for $n=2$ the uncertainty due to the

respond to relaxed constituents, the small core level shift due to strain[66] is neglected. If one is interested in the case where

band edge energy of each chalcopyrite needs to be shifted

size and direction of the strain through the deformation

terms of Eq. (6),[66] while the shift in the third term is expected to be small.[66]

A. Mixing enthalpy

can be obtained from the calculated alloy total energies as

$$\Delta H(x=1/2)=E_{\rm tot}(ABA_2/A_2B_2A_2)-E_{\rm tot}(ABA_2)$$

Our calculated results are denoted as ΔH in Fig. 2. We find that for both mixed-anion and mixed-cation alloys the mixing enthalpy is positive and increases as the lattice mismatch

ΔH(S,Te) are 3, 13, and 41 meV/atom, respectively, while

spectively. The positive sign of ΔH indicates that here, the ground state at $T=0$ corresponds to phase separation into the pure chalcopyrite constituents. (However, at finite temperatures, the disordered phase can be stabilized through en-

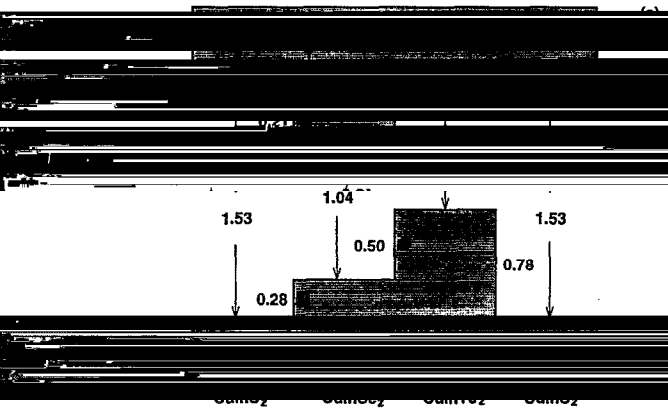

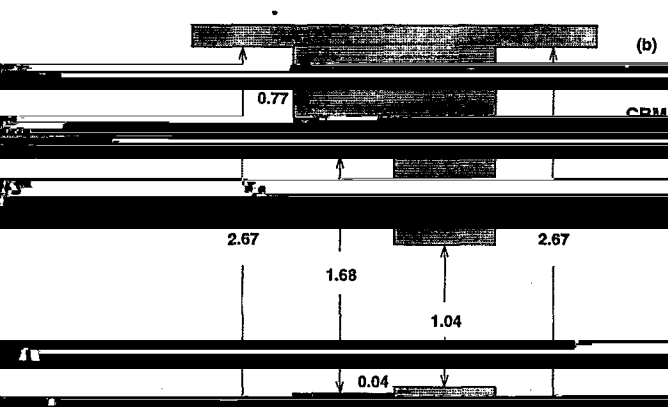

FIG. 4. Calculated intrinsic valence-band and conduction-band offsets for common-anion chalcopyrite compounds. The values pertain to fully relaxed components having their free-space equilibrium structures.

FIG. 5. Calculated intrinsic valence-band and conduction-band offsets for interfaces between Zn-based II-VIs. The values pertain to fully relaxed components having their free-space equilibrium structures.

B. Band offsets

4(a)], and between the three common-anion $CuAlSe_2/CuGaSe_2/CuInSe_2$ chalcopyrites [Fig. 4(b)]. For comparison, we have also calculated the intrinsic valence-band offsets between the II-VI ZnS/ZnSe/ZnTe chalcogenides (Fig. 5). The conduction band offsets ΔE_c are ob-

band lineup is "type II." This is true both in II-VIs and in chalcopyrites. For the S/Te interface, the lineup is type II in chalcopyrites and type I in II-VIs. However, strain may

and (Al,Ga) chalcopyrite alloys, and is slightly larger for

(ii) For common-cation chalcopyrites [Fig. 4(a)] the

range at finite temperatures. The mixing enthalpy ΔH is large for the (S,Te) alloy, suggesting that large miscibility gap can exist in this system.[16]

We have also calculated the mixing enthalpy for mixed-

(S,Te). For these Zn alloys the equilibrium structural parameters are determined using the valence force field (VFF) model.[52,53] We find that the mixed-anion chalcopyrite alloys

sponding Zn alloys (Fig. 3). This is consistent with the observation that the chemical disparity between the alloyed elements is reduced in chalcopyrites relative to the II-VI alloys (see Secs. III B and III E below) and that chalcopyrites have smaller bond bending force constants, thus, smaller elastic

the valence-band offsets for these systems mainly reflect the differences between anion p orbital energies. The atomic p orbital energies increase from S to Se to Te (Table V). The large conduction-band offset is partly due to the anion s or-

that the CBM energy moves up as the volume of the compound decreases.

(iii) The valence band offsets between common-cation

responding II-VIs (Fig. 5). The reason is the larger $p-d$ repulsion in chalcopyrites: the $p-d$ repulsion is inversely proportional to the energy difference between the cation d and anion p state.[63,64,69] In the chalcopyrite and II-VI compounds the cation d bands are below the anion p bands.[3]

TABLE V. Calculated (semirelativistic) atomic LDA valence orbital energies ϵ_{s}, ϵ_{p}, and ϵ_{d} (in eV) of the elements studied in this paper.

Al	−7.91	−2.86	
Ga	−9.25	−2.82	−19.18
In	−8.56	−2.77	−18.75
Cu	−4.95		−5.39
Zn	−6.31	−1.31	−10.49

Cu d level. Since the p orbital energy decreases from Te to Se to S, the p-d repulsion is stronger in sulphides than in selenides and tellurides, and the upward shift of the VBM is

p orbitals and thus the valence-band offset. This effect is weaker in II-VI systems than in the chalcopyrite systems, the band offset due to the $p-d$ repulsion is larger in the chalcopyrite systems.

(v) For common-anion chalcopyrites [Fig. 4(b)] we find anion rule[70] (which states that since the VBM is primarily a bonding anion p state, the valence-band offset for the common-anion system should be small) is followed rather well for this system. Although this rule holds in some cases (e.g., GaV/InV, $\Delta E_v \sim 0.1$ eV), it does not holds in other cases (e.g., AlV/GaV and AlV/InV, where the band offset $\Delta E_v \sim 0.5$ eV for V=P, As, and Sb).[71] The breakdown of the common-anion rule in zinc-blende systems (e.g., AlAs/GaAs) is attributed[62–64] to the coupling between anion and cation d orbitals. For GaAs the cation d bands are below the anion p bands, hence $p-d$ repulsion pushes the VBM up. On the other hand, in AlAs the empty cation d bands are VBM down. Thus, the VBM of GaAs is higher in energy than AlAs. The same $p-d$ coupling effect exists in the Cu-based chalcopyrite compounds. However, in chalcopyrites half of the cation sublattice is occupied by Cu atoms and thus expects that the valence band offset in chalcopyrites will be about half the values in the corresponding III-V system.

(v) We find that for both common-cation and common-

compound and a chalcopyrite compound, our present results can be combined with our earlier studies[65,69] of the band

II-VI compound. For example, our calculated ΔE_v between $CuInSe_2$ and CdS is 1.07 eV, hence we expect that ΔE_v between $CuInSe_2$ and CdSe should be 0.28 eV and that ΔE_v

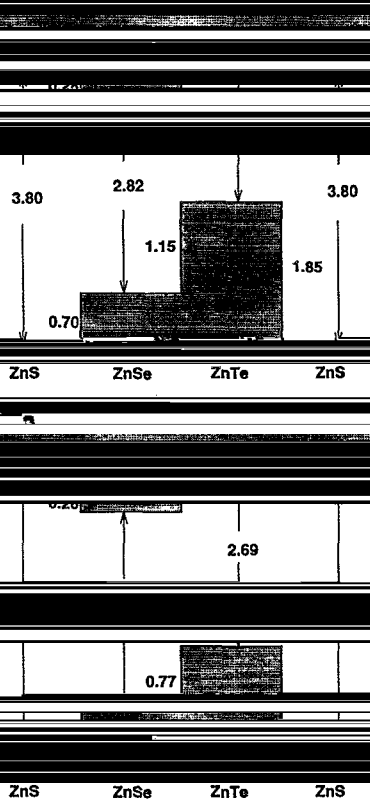

FIG. 6. Calculated valence-band and conduction-band offsets between Zn-based II-VIs strained on a GaAs(001) substrate: (a) lineups for hh states and

between $CuInS_2$ and CdS should be 0.79 eV. In some cases (e.g., $CuIn_xGa_{1-x}Se_2$) one may also assume that the VBM of

hence one can estimate the band offset between a chalcopyrite *alloy* and a II-VI compound.

(vi) Using the pseudopotential method, Nakayama[73] has $\Delta E_{v,hh}$ between different Zn-based II-VI semiconductors strained on a GaAs(001) substrate. He found that $\Delta E_{v,hh}$ between ZnS/ZnSe, ZnSe/ZnTe, and ZnS/ZnTe are 0.86, 1.29, and 2.15 eV, respectively. These values are larger than (Fig. 5) obtained for the *relaxed* interface. The larger values of Nakayama are partly due to strain. To compare our all-electron results with the (no−d) pseudopotential results of

sets of the *strained superlattice* using the procedure de-

part b) band lineups between the strained Zn-based II-VI semiconductors. The hh and lh levels are degenerate for re-

1.85 eV, respectively. These are 0.16, 0.14, and 0.30 eV smaller than Nakayama's values.[73] $\Delta E_{v,hh}$ increases relative to the relaxed superlattices, since the hh energy increases

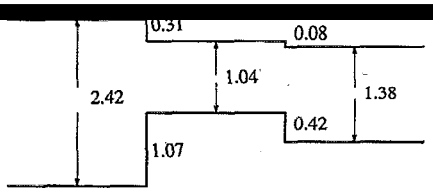

TABLE VI. Calculated and the *most reliable* experimental (see references in [illegible]) values of [illegible] for the [illegible] also given for comparison.

Alloy	Calculated	Experiment	Tinoco *et al.*[a]
$Cu(Al,Ga)Se_2$	0.39	0.28	0.06
$Cu(Ga,In)Se_2$	0.21	0.15–0.24	0.18
$Cu(Al,In)Se_2$	0.59	···	0.24
$CuIn(S,Se)_2$	0.04	~0.0	0.10
[illegible]	[illegible]	[illegible]	[illegible]

[a]Ref. 80.

almost linearly with the epitaxial strain along the (001) direction.[67] It is interesting to see that for the ZnS/ZnTe interface, the system changes from type I for a relaxed interface (Fig. 5) to type II for a strained interface [Fig. 6(a)]. This is because under strain the CBM energy of ZnTe increases, while that of ZnS decreases. Our calculated ΔE_c are given in Fig. 6. The band gap of the compounds also changes with strain, e.g., we find that for the strained ZnTe compound, the band gap is reduced by 0.09 eV. (Note, however, [illegible] rather than epitaxially strained values to derive the conduction-band offsets. This can cause errors in his calculation of ΔE_c.)

(vii) There are a few indirectly measured values of ΔE_v(ZnSe/ZnTe): (a) Based on fitting the dominant photoluminescence peaks to the $ZnSe_xTe_{1-x}$/ZnTe superlattice band structure obtained by $\mathbf{k}\cdot\mathbf{p}$ theory, Rajakarunanayake *et al.*[74] deduced a value for the unstrained valence-band offset ΔE_v(ZnSe/ZnTe)=0.91±0.12 eV. This fitting assumed that the observed peak energy corresponds to band edges transition. If the photoluminescence originates instead from (below-the-band-edge) exciton-like transition, the fitted [illegible] smaller.[74] (b) Recently, capacitance-voltage measurement by Ukita *et al.*[75] of a Schottky-like heterojunction barrier gave ΔE_v(ZnSe/ZnTe)=0.7–0.8 eV. Both experimental results[74,75] agree very well with our calculated value of 0.73 eV (Fig. 5). However, recent pseudopotential calculation of Freytag[76] treating the Zn 3d states as frozen core found a much larger value of the band offset ΔE_v(ZnSe/ZnTe)=1.09 eV. This dis[illegible] neglect of explicit $p-d$ coupling in the latter. Recall that $p-d$ repulsion raises the energy of VBM in inverse proportion to the $p-d$ energy difference. The effect is thus larger [illegible]

(viii) Recently, Schmid *et al.*[77] found that between the CdS and $CuInSe_2$ layers in CdS/$CuInSe_2$ solar cells there exists a $CuInSe_2$-derived Cu-poor "ordered vacancy compound" (OVC). We have studied[78] the band alignment between CdS and the OVC $CuIn_5Se_8$. Our calculated band [illegible] CdS/$CuInSe_2$ interface are also included in Fig. 7 for comparison. We find from our calculation that the unstrained [illegible] This is due to stronger $p-d$ coupling in the former. The calculated band gap of $CuIn_5Se_8$ is 0.34 eV larger than for $CuInSe_2$, so the CBM of $CuIn_5Se_8$ is 0.08 eV lower than for [illegible] OVCs can be formally written as an alloy in the form $(CuIn_5Se_8)_{1-x}(Cu_4In_4Se_8)_x$. Hence, the band alignment between any of these OVCs and $CuInSe_2$ can be linearly interpolated from the values given in Fig. 7. For instance, for the [illegible] are 0.34 and 0.06 eV lower than $CuInSe_2$, respectively.

C. Bowing in chalcopyrite alloys

The optical bowing parameter b of the chalcopyrite alloy is given by

$$b=-4\left[E_g(ABX_2/A'B'X_2')-\frac{1}{2}E_g(ABX_2)-\frac{1}{2}E_g(A'B'X_2')\right]. \quad (12)$$

Note that both computational and LDA errors[79] tend to cancel in Eqs. (10) and (12), since we compare chemically identical systems in two different forms: the $ABX_2/A'B'X_2'$ alloys vs. equivalent amounts of the constituents ABX_2 and $A'B'X_2'$. Figure 2 gives the calculated bowing parameter for stoichiometric mixed-anion [Fig. 2(a)] and mixed-cation [Fig. 2(b)] chalcopyrite alloys. Comparing our calculated re[illegible] we next comment on the *experimental* results, so as to decide with what data to compare our calculations. The experimental results of Aven *et al.*,[18] yielding *negative* bowing [illegible] $CuIn(S,Se)_2$ and $Cu(Ga,In)Se_2$ are also in disagreement with other measurements. Samanta *et al.*[13] have recently presented bowing parameters for eight chalcopyrite alloys (Table I). We see that some of their results, yielding zero and [illegible] *et al.*[19] suggested that bowing for mixed-cation alloys is small[19] ($b<0.05$ eV). This is not supported by other experi[illegible] tering of the experimental data (Table I) could reflect

nonstoichiometry[30] in the samples. Table VI collects the measured bowing parameters that we assess as being the most reasonable at this time.

To fit the experimental data for optical bowing of chalcopyrite alloys in which A and B are the mixed atoms, Ti-

$$b(A,B)=5/4|\chi_A-\chi_B|, \tag{13}$$

where χ_α is Phillip's electronegativity[81] for atom α. Their results are also listed in Table VI for comparison. Although their formula ... coefficients fo... loys used in their fitting [(Ga,In), (S,Se), and (Se,Te)], this formula underestimates the bowing of the *other* alloy systems, (Al,Ga), (Al,In), and (S,Te). For example, their pre-

(0.6 eV). This suggests that the formula of Tinoco *et al.* cannot be reliably extended to systems not used in their fitting. Furthermore, the phenomenological scaling of Eq. (13) does ... if the ... nor does it explain the different bowing of chalcopyrites [e.g., $CuGa(S,Se)_2$] versus zinc-blende [Zn(S,Se)] alloys. This will be discussed in Sec. III E below.

D. Bowing in Zn-based II-VI alloys

... the optical bowing, we have calculated the bowing coefficient for Zn-based II-VI alloys. Figure 3 gives our calculated ... good. We notice that bowing parameters measured from molecular beam epitaxy (MBE) grown films[39,41] have large values suggesting that those samples may not be perfectly random (see below).

The results $b=2.71$ eV for Zn(S,Te) can be compared with the value $b=2.94$ eV obtained by Bernard and Zunger[61] using a linear superposition of band gaps of

$$E_g(1/2)\simeq\tfrac{1}{2}[E_g(ZnS_nTe_{4-n})+E_g(ZnS_{4-n}Te_n)], \tag{14}$$

ZnS_nTe_{4-n} at $x=1/2$. For Zn(S,Se) and Zn(Se,Te) Bernard and Zunger[61] used in Eq. (14) only the $n=2$ data, finding $b=0.39$ eV and $b=1.96$ eV, to be compared with the more accurate current values of $b=0.50$ eV and $b=1.14$ eV, respectively.

Comparing now the bowing in mixed-anion chalcopyrites [Fig. 2(a)] with that in mixed-anion Zn chalcogenides (Fig. 3) we see the same trend $b(S,Se)<b(Se,Te)<b(S,Te)$, relative to the II-VI zinc-blende alloys. This trend is analyzed in the next section.

E. Analysis of bowing coefficients

Optical bowing in semiconductor alloys is caused by the difference of volume deformation potentials of the constituents. ... alloy potential and the average potential of the constituents.

For direct band-gap semiconductors, the top of the valence band is mostly an anion p like state (with some cation p and d characters), while the bottom of the conduction band is mostly a cation s and anion s state. The ΔV-induced *intraband* coupling within the conduction band and within the ... ents. On the other hand, ΔV-induced *interband* coupling between the conduction and the valence bands lowers the VBM and raises the CBM, thus *increasing* the band gap. For most ... of the same orbital character is much stronger than the interband coupling, so alloying reduces the band gap and the ... and b, and a component due to the size mismatch between the A and B atoms. When two compounds have large difference in their atomic potential or large difference in their size, the optical bowing is expected to be large. The atomic po-

the differences of their atomic valence eigenvalues. In Table V we show our calculated LDA atomic valence eigenvalues ϵ_s, ϵ_p, and ϵ_d of elements studied in this paper. The size mismatch of the constituents can be inferred from the mismatch of their lattice constants.

... mixed-anion alloys studied here [Fig. 2(a)], CuIn(S,Se) has a rather small bowing, while the bowings for CuIn(Se,Te) and CuIn(S,Te) are large. This is because (i) the s chemical potential difference between S and Se is small (~0.2 eV), while the Te s potential is about 2 eV higher than the one for S and Se (Table V), (ii) the p chemical potential difference is smaller between S and Se (~0.45 eV) than between S and Te (~1.0 eV), and (iii) the size mismatch between S and Se is ... $b(S,Se)<b(S,Te)<b(Se,Te)$ ... alloys also causes wave-function localization. We find that in CuIn(S,Te) the top of the valence band is strongly localized on the Te atom with higher p orbital energy, while the bottom of the conduction band is strongly localized on the S atom with low s orbital energy. No strong wave-function localization is observed in CuIn(S,Se), which has almost no bowing. The significant *reduction* in bowing in the chalcopyrites relative to the zinc-blende alloys can be understood by ... reduces their valence-band offset (hence, chemical disparity) more than the Zn chalcogenides (Sec. III B), thus reduces the bowing.

In *mixed-cation alloys* [Fig. 2(b)] most of the level re- ... their relatively large band offset, the $Cu(Al,Ga)Se_2$ and $Cu(Al,In)Se_2$ alloys also exhibit significant perturbation in ... =0.39 and 0.59 eV, respectively) than $Cu(Ga,In)Se_2$ (b

TABLE VII. Calculated (top four lines) bowing parameters of Zn chalco-

Phase	Zn(S,Se)	Zn(Se,Te)	Zn(S,Te)
b(CH)	0.10	0.25	0.61
b(CuPt)	1.09	3.15	5.93
b(random)	0.50	1.14	2.71
b_{expt}(random)	~0.50	1.23–1.50	3.0–3.2

=0.21 eV). We also notice that the bowing coefficient of $Cu(Ga,In)Se_2$ is smaller than (Ga,In)V (with V=P, As, and Sb) alloys (b~0.5 eV).[6] This is because in the chalcopyrite system half of the cation sites are occupied by Cu, so the

copyrite alloys is reduced relative to zinc-blende alloys. For the $Cu(Al,Ga)Se_2$ and $Cu(Al,In)Se_2$ alloys the chemical disparity and size disparity between Al and Ga, and between Al

for these two alloys.

Our foregoing discussion centered on the SQS models

bowing to those found for hypothetical small unit cell *ordered* alloys. Our results for Zn chalcogenides in the ordered CuAu (an AB superlattice along [001] direction), chalcopyrite and CuPt (an AB superlattice along [111] direction) structures are summarized in Table VII. We see that band gaps (or bowing) depend sensitively on the assumed atomic

dered phases,[82] the bowing of the ordered phases has the following trend

$$b_{CuPt} > b_{CuAu} > b_{CH}, \tag{15}$$

$$b_{CuPt} > b_{Random} > b_{CH}. \tag{16}$$

These trends are also found in calculations

that if an alloy orders into the CuPt structure, its band gap will be drastically reduced relative to the disordered alloy.[83] In Zn(S,Se), Zn(Se,Te), and Zn(S,Te) alloys, CuPt ordering at x=1/2 can reduce the band gap by up to 0.15, 0.50, and 0.81 eV, respectively, relative to the random alloy. For alloys ordering into the chalcopyrite structure, the band gap is in-

The same trends of Eqs. (15) and (16) are found in chal-

bowing parameter b=1.25 eV when the Se and Te atoms were arranged in the ordered CuAu structure, while b=0.17 eV when the Se and Te were arranged in the ordered chalcopyrite structure. These results differ significantly from the

ture.

IV. SUMMARY

studied systematically the (i) alloy mixing enthalpies ΔH,

(iii) alloy bowing coefficients b for three mixed-anion

M=Al,Ga,In) chalcopyrite alloys. The random chalcopyrite alloys are represented by an SQS model. We find that (i) for all the chalcopyrite alloys studied here the mixing enthalpy is positive, indicating that for these alloys the ground state at T=0 corresponds to phase separation into the pure chalcopyrite constituents. However, at higher temperature, the disordered phase can be stabilized through entropy. The mixing enthalpy ΔH is rather small for (S,Se), (Al,Ga), (Se,Te), and (Ga,In) alloys, suggesting that these alloys will be miscible in the whole composition range and can thus be formed easily. The mixing enthalpy ΔH is large for the (S,Te) alloy, suggesting that a large miscibility gap can exist in this system. (ii) For mixed-cation interfaces, most of the band offsets occur in the conduction band, while for mixed-anion interfaces both ΔE_c and ΔE_v are large. (iii) The calculated

and are in good agreement with the most reliable experimental data for stoichiometric alloys. CuIn(S,Te) and CuIn(S,Te) alloys have a large bowing coefficient due to the

(iv) The difference of bowing coefficients and band offsets

corresponding zinc-blende systems are explained in terms of the larger $p-d$ coupling in chalcopyrite systems. Bowing parameters for ordered Zn chalcogenide alloys (in CuAu, CuPt, and chalcopyrite structure) are predicted. The band alignment between $CuInSe_2$ and $CuInSe_2$-derived ordered vacancy compounds are also presented.

ACKNOWLEDGMENTS

We thank Professor L. G. Ferreira for verifying the SQS structure for the mixed-cation chalcopyrite alloy. This work

No. DE-AC02-83-CH10093.

(1987).
[3] J. E. Jaffe and A. Zunger, Phys. Rev. B **28**, 5822 (1983).
[4] J. E. Jaffe and A. Zunger, Phys. Rev. B **29**, 1882 (1984), and references therein.
[5] J. K. Furdyna, J. Appl. Phys. **64**, R29 (1988), and references therein.
[6] *Landolt-Bornstein: Numerical Data and Functional Relationships in Science and Technology*, edited by O. Madelung, M. Schulz, and H. Weiss
[7] J. Hedstrom, H. J. Olsen, M. Bodegard, A. Kylner, L. Stolt, D. Hariskos,
[8] A. M. Gabor, J. R. Tuttle, D. S. Albin, M. A. Contreras, R. Noufi, and A. M. Hermann, Appl. Phys. Lett. **65**, 198 (1994).
[9] For a review of device properties, see A. Rothwarf, Solar Cells **16**, 567 (1986).
[10]
51, 551 (1990).

[12] S. Shirakata, A. Ogawa, S. Isomura, and T. Kariya, Jpn. J. Appl. Phys. Technol. **28**, 1175 (1993).
[14] G. H. Chapman, J. Showchun, J. J. Loferski, R. K. Garside, and R. Beau
[15] I. V. Bodnar, B. V. Korzun, and A. I. Lukomskii, Phys. Status Solidi B **105**, K143 (1981).
[16] M. Quintero and J. C. Woolley, J. Appl. Phys. **55**, 2825 (1984).
1305.
[18] J. Avon, K. Yoodee, and J. C. Woolley, Nuovo Cimento D **2**, 1858 (1983).
[19] S. Chatraphorn, T. Panmatarite, S. Pramatus, A. Prichavudhi, R. Kritayakirana, J.-O. Berananda, V. Sa-yakanit, and J. C. Woolley, J. Appl. Phys. **57**, 1791 (1985).
[20] M. Quintero, R. Tovar, E. Guerrero, F. Sanchez, and J. C. Woolley, Phys. Status Solidi A **125**, 161 (1991).
[21] P. Grima, M. Quintero, C. Rincon, and J. C. Woolley, Solid State Commun. **67**, 81 (1988).
[22] N. Tsuboi, S. Kobayashi, F. Kaneko, and T. Maruyama, Jpn. J. Appl. Phys. **27**, 972 (1988).
Isomura, Jpn. J. Appl. Phys. **32**, L1304 (1993).
k31 (1982).
[26] T. F. Ciszek, R. Bacewicz, J. Durrant, S. K. Deb, and D. Dunlavy, *Pro-*
(MRS, Pittsburgh, 1987), p. 155.
the 19th IEEE PV Specialists Conference (IEEE, New York, 1987), p.
Mickelsen, *Proceedings of the 19th IEEE PV Specialists Conference* (IEEE, New York, 1987), p, 1445.
[32] T. Yamaguchi, J. Matsufusa, and A. Yoshida, Jpn. J. Appl. Phys. **31**, L703 (1992).
[33] C. Larez, C. Bellabarba, and C. Rincon, Appl. Phys. Lett. **65**, 1650 (1994).
[34] L. G. Suslina, D. L. Fedorov, S. G. Konnikov, F. F. Kodzhespirow, A. A. Andreev, and E. G. Shariai, Fiz. Tekh. Poluprovodn. **11**, 1934 (1977) [Sov. Phys. Semicond. **11**, 1132 (1977)].
80, 378 (1979); D. Ecelnie, M. de Murcia, and G. Bougnot, Thin Solid Film **70**, 285 (1980).
[36] P. Mach, P. Flegel, L. G. Suslina, A. G. Arashkin, J. Meese, and G. Voigt
T. El Shair, and A. M. Ebrahim, Appl. Phys. A **36**, 51 (1985).
[38] A. Ebina, M. Yamamoto, and T. Takahashi, Phys. Rev. B **6**, 3786 (1972).
R. J. Martin, Appl. Phys. Lett. **58**, 2509 (1991).
[40] R. Hill and D. Richardson, J. Phys. C **6**, L115 (1973).
J. Sham, *ibid.* **140**, A1133 (1965).
[45] K. A. Mader and A. Zunger, Appl. Phys. Lett. **64**, 2882 (1994); Phys. Rev. B (to be published).
[46] J. M. Sanchez, F. Ducastelle, and D. Gratias, Physica **182A**, 334 (1984).
Phys. Rev. B **42**, 9622 (1990).
[48] R. Magri, S. Froyen, and A. Zunger, Phys. Rev. B **44**, 7947 (1991).
[49] S.-H. Wei and A. Zunger, Phys. Rev. B **43**, 1662 (1991); 14272 (1991).
[50] Z. W. Lu, S.-H. Wei, and A. Zunger, Phys. Rev. B **44**, 10470 (1991).
[51] Z. W. Lu, S.-H. Wei, and A. Zunger, Phys. Rev. B **45**, 10314 (1992).
[52] P. N. Keating, Phys. Rev. **145**, 637 (1966).
[53] J. L. Martins and A. Zunger, Phys. Rev. B **30**, 6217 (1987).
[54] L. Vegard, Z. Phys. **5**, 17 (1921).
[55] H. W. Spiess, V. Haeberln, G. Brandt, A. Rauber, and J. Schneider, Phys. Status Solidi B **62**, 183 (1974).
[56] S.-H. Wei and H. Krakauer, Phys. Rev. Lett. **55**, 1200 (1985), and references therein.
[59] S. Froyen, Phys. Rev. B **39**, 3168 (1989).
[60] J. J. Hopfield, J. Phys. Chem. Solids **15**, 97 (1960).
Scientific, Singapore, 1993).
F. H. Pollak and M. Cardona, Phys. Rev. **172**, 816 (1968).
[68] C. G. Van de Walle, Phys. Rev. B **39**, 1871 (1989).
[69] S.-H. Wei and A. Zunger, Appl. Phys. Lett. **63**, 2549 (1993).
[72] A. D. Katnani and G. Margaritondo, J. Appl. Phys. **54**, 2522 (1983).
[73] T. Nakayama, J. Phys. Soc. Jpn. **61**, 2434 (1992).
[74] Y. Rajakarunanayake, M. C. Phillips, J. O. McCaldin, D. H. Chow, D. A. Collins, and T. C. McGill, Proc. SPIE **1285**, 142 (1990).
[75] M. Ukita, F. Hiei, K. Nakano, and A. Ishibashi, Appl. Phys. Lett. **66**, 209 (1995).
2902 (1993).
[78] S.-H. Wei and A. Zunger (unpublished).
1973).
[82] S.-H. Wei and A. Zunger, Phys. Rev. B **39**, 3279 (1989).
[84] M. A. Ryan, M. W. Peterson, D. L. Williamson, J. S. Frey, G. E. Maciel, and B. A. Parkinson, J. Mater. Res. **2**, 528 (1987).